



## Research Article

# Comparative evaluation of mechanical performance of steel slag and earthen granular aggregates

Aslı YALÇIN DAYIOĞLU<sup>\*,1</sup>, Mustafa HATİPOĞLU<sup>1</sup>, Ahmet H. AYDİLEK<sup>2</sup>

<sup>1</sup>Istanbul Technical University, İstanbul, Türkiye

<sup>2</sup>University of Maryland, College Park, MD, USA

## ARTICLE INFO

### Article history

Received: 20 February 2023

Revised: 20 March 2023

Accepted: 02 April 2023

### Key words:

Steel slag; sustainability, resilient modulus, permanent deformation

## ABSTRACT

The diminishing quantity of natural resources has resulted in a search for alternative materials. Reusing industrial by-products, such as steel slag, provides opportunities for sustainable highway construction practices due to the valuable space they occupy and the potential environmental impacts when they are stockpiled. In this paper, the mechanical suitability of steel slag as an unbound highway aggregate is investigated, and its performance is compared with that of traditional graded aggregate base (GAB) materials. In order to compare the behavior, three steel slag samples with different aging properties and five aggregate samples from different quarries were employed. The results indicate that resilient moduli and permanent deformation characteristics of steel slag are comparable with those of traditional aggregates and can replace when used as a base or subbase course.

**Cite this article as:** Yalçın Dayıoğlu, A, Hatipoğlu, M., & Aydılek, A. (2023). Comparative evaluation of mechanical performance of steel slag and earthen granular aggregates. *J Sustain Const Mater Technol*, 8(1), 12–19.

## 1. INTRODUCTION

Stockpiling large quantities of steel slag, a by-product of steel production, has become an issue over the years as the practice takes valuable space in urban areas and may result in the leaching of undesired compounds into surface waters or groundwater [1, 2]. Thus, alternative applications for the use of steel slag need to be evaluated. Steel slag constitutes approximately 15% of 1 ton of steel produced, and in 2021 was estimated to total 190–280 million tons globally and 9 million tons in the United States [3]. Using steel slag in various applications, such as clinker cement aggregate or recycling in iron-making applications, has been extensive-

ly studied [4–11]. In addition, using steel slag in highway applications has been a very good research topic due to the consumption of larger volumes of the material [12]. Investigated the use of electric arc furnace (EAF) steel slag as an unbound granular aggregate for low-volume roads and showed that steel slag might have California Bearing Ratio (CBR) values up to 200%, and its resilient modulus is much higher than those of traditional aggregate materials. Various studies [13–16] evaluated the performance of EAF slag when used as an asphalt aggregate and showed that the mechanical performance of steel slag was comparable to that of natural aggregates. Ameri et al. [17] mixed steel slag with virgin aggregate and indicated that steel slag enhances the

\*Corresponding author.

\*E-mail address: yalcinas@itu.edu.tr



quality of cold-in-place-recycled asphalt mixtures. Maghool et al. [18] evaluated the mechanical and environmental impacts of EAF steel slag when used on highways and found that, especially when blended with a fine-grained material, EAF slag would have excellent mechanical characteristics to be used as a base layer.

Steel slag has high CaO and MgO content due to the composition of the fluxing agents used to purify the material, which results in the formation of calcium hydroxide (Ca(OH)<sub>2</sub>) upon reacting with water which ultimately causes volumetric expansion [19–21]. Past studies by Ozkok et al. [22] assessed the success of different mitigation methods, such as bitumen coating, bathing steel slag in either Fe(III), Al(III), or PO<sub>4</sub>(-III), and mixing steel slag with an alum-based drinking water treatment residual (WTR), and showed that WTR amendment proved to be the most effective method. However, Ca release was also reduced by about 50- 70% for the other methods. Steel slag can also be mixed with WTR to reduce the ultimate swelling potential [23] significantly. Similarly, studies conducted by [1, 2] revealed that when encapsulated by a clayey soil layer and/or by the presence of a clayey natural subgrade, both trace metal leaching and swelling potential of water treatment residual (WTR) treated basic oxygen furnace (BOF) steel slag are mitigated.

In order to evaluate the potential use of steel slag in highway base applications, a definition of its structural stability through resilient modulus tests is necessary. The test provides an essential input parameter for the pavement design, aligned with the mechanistic-empirical pavement design guidelines (MEPDG) to design flexible pavements [24]; however, high constant stresses are usually not applied on the materials for a very long period during the test, while they are being exposed to such stresses during their service life. Thus, permanent deformation tests are generally per-

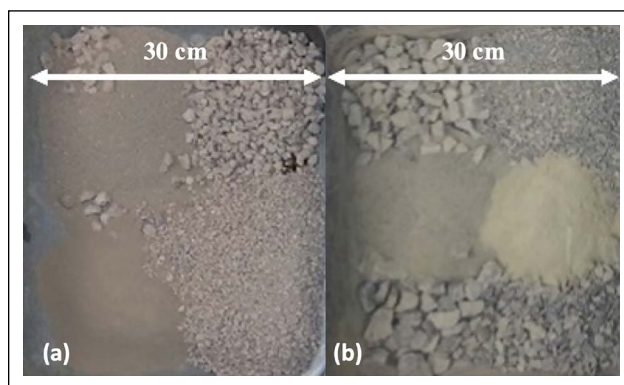


Figure 1. Materials used in this study (a) Steel Slag; (b) GAB Material.

formed on unbound granular aggregates to determine their plastic deformation (rutting) potential [25–28].

The main goal of this study was to evaluate the stiffness and plastic deformation characteristics of steel slag and to compare them with those of graded aggregate base (GAB) materials. For this purpose, laboratory resilient modulus and permanent deformation tests were conducted on pure steel slag and GAB samples. In order to study the nonlinear behavior of steel slag and GAB materials, the model recommended by mechanistic-empirical pavement design guidelines (MEPDG) was employed. Furthermore, permanent deformation tests were performed on specimens with up to 10,000 load repetitions to determine the steel slag's plastic strain and compare its performance with natural aggregates.

## 2. MATERIALS

Three steel slag (S) materials with different aging properties (i.e., six months (S6M), one year (S1Y), and 2+ years (S2Y)) and five different graded aggregate base (GAB) ma-

Table 1. Gradation properties of the materials tested

Material	Gravel (%)	Sand (%)	FC (%)	D <sub>60</sub> (mm)	D <sub>30</sub> (mm)	D <sub>10</sub> (mm)	C <sub>u</sub>	C <sub>c</sub>	Passing from 2-mm sieve (%)	Passing from 0.42-mm sieve (%)
S6M	35	53.5	11.5	4	0.65	0.07	57	1.5	46	25
S1Y	22.3	68.6	9.1	2.5	0.64	0.08	31	2	53	25
S2Y	20.7	67	12.3	2.5	0.55	0.045	53	2.7	54	27
GAB1	58	36	6	9.8	1.6	0.1	98	2.6	32	17
GAB2	46.8	44.6	8.6	6.7	0.5	0.085	79	0.44	44	28
GAB3	61	33	6	10.1	2	0.15	67	2.64	30	19
GAB4	58	36.7	5.3	10.1	1.5	0.15	67	1.49	34	16
GAB5	56	36	8	10.0	1.2	0.09	111	1.6	30	15
AASHTO (UL)	45	47	8	NA	NA	NA	NA	NA	NA	NA
AASHTO (LL)	65	35	0	NA	NA	NA	NA	NA	NA	NA

Note: S: Steel slag, GAB: Graded Aggregate Base, FC: Fines Content. NA: Not available. Cu: Coefficient of uniformity Cc: Coefficient of curvature, UL: Upper Limit, LL: Lower Limit. Values outside of the AASHTO Limits are in bold.

**Table 2.** Physical and chemical properties of the materials tested

Material	Physical properties						Chemical properties			
	Gs	I <sub>p</sub> (%)	w <sub>opt</sub> (%)	γ <sub>dry-max</sub> (kN/m <sup>3</sup> )	USCS classification	AASHTO classification	SiO <sub>2</sub> (%)	Al <sub>2</sub> O <sub>3</sub> (%)	Fe <sub>2</sub> O <sub>3</sub> (%)	CaO (%)
S6M	3.46	NP	10	23.9	SW-SM	A-1-b	11.48	4.10	36.45	32.84
S1Y	3.45	NP	11	22.5	SW-SM	A-1-b	12.18	3.68	35.93	32.42
S2Y	3.45	NP	13.5	22.2	SW-SM	A-1-b	11.65	3.60	37.12	32.41
GAB1	2.77	NP	5.8	23.9	GW	A-1-a	60.9	13.3	9.43	2.93
GAB2	2.79	NP	4.2	23.9	GW	A-1-a	44.1	3.04	1.57	26.8
GAB3	3.01	NP	5.3	24.8	GW	A-1-a	47.7	15.6	11.0	11.9
GAB4	2.68	NP	4.7	23.0	GW	A-1-a	11.9	1.95	0.85	31.7
GAB5	2.79	NP	5.2	23.4	GW	A-1-a	2.36	0.70	1.31	29.3

Note: I<sub>p</sub>: plasticity index, Gs: specific gravity NP: non-plastic, w<sub>opt</sub>: optimum moisture content, γ<sub>dry-max</sub>: maximum dry unit weight.

materials were included in the testing program (Fig. 1). The GAB and S materials were collected from different quarries in the eastern part of the United States and tested in the laboratory. Both materials contained coarse and non-plastic fine fractions. The gradation properties of the materials are provided in Table 1, whereas the index properties are given in Table 2.

The fines fraction of GAB and S are 5.3–8.6% and 9.1–12.3% by weight, respectively. Gradation properties of all three steel slag materials exceed the AASHTO M147 upper level for base aggregates. However, it should be noted that those specifications were developed for traditional GAB materials, and no specific limits were set for steel slag. The unit weight of GAB materials varies between 2.68 and 3.01 and agrees with the values reported by [29, 30]. The higher specific gravity of the slags as compared to earthen aggregates can be attributed to their higher Fe<sub>2</sub>O<sub>3</sub> content (35.93–37.12% versus 0.85–11.0, Table 2), and previous studies reported comparable specific gravities for steel slag samples [31, 32]. GAB materials utilized in the current study were classified as A-1-a according to AASHTO, while the S materials were classified as A-1-b [33].

Slag particles' bituminous coating (BC) was achieved using an asphalt binder PG-64-22. The physical properties of the asphalt binder can be found in [34]. The asphalt binder (Gs= 3.45) is solid at room temperature and is viscous fluid at 90°C. Steel slag particles were mixed with 4% by-weight asphalt binder following the procedures outlined in [34].

### 3. METHODS

#### 3.1. Resilient Modulus Test

The resilient modulus test is usually performed to obtain soil stiffness under confining stress and a repeated axial load. All the resilient moduli tests were performed by AASHTO T-307, a protocol for testing highway base and subbase mate-

**Figure 2.** Resilient modulus test setup.

rials [35]. The loading sequences used in the resilient modulus test are presented in Table 3. A vibratory compactor was used to place all GAB and S specimens in split molds with a diameter of 152 mm and a height of 305 mm per ASTM

Table 3. Testing sequences used for materials in this study (AASHTO T-307)

Sequence no	Confining pressure	Maximum deviatoric stress	Cyclic stress	Constant stress	No of repetitions
0 (Conditioning)	103.4	103.4	93.1	10.3	500
1	20.7	20.7	18.6	2.1	100
2	20.7	41.4	37.3	4.1	100
3	20.7	62.1	55.9	6.2	100
4	34.5	34.5	31.0	3.5	100
5	34.5	68.9	62.0	6.9	100
6	34.5	103.4	93.1	10.3	100
7	68.9	68.9	62.0	6.9	100
8	68.9	137.9	124.1	13.8	100
9	68.9	206.8	186.1	20.7	100
10	103.4	68.9	62.0	6.9	100
11	103.4	103.4	93.1	10.3	100
12	103.4	206.8	186.1	20.7	100
13	137.9	103.4	93.1	10.3	100
14	137.9	137.9	124.1	13.8	100
15	137.9	275.8	248.2	27.6	100

Table 4. Resilient modulus and permanent deformation test results

Material	SM <sub>R</sub> (MPa)	Fitting parameters			R <sup>2</sup>	ε <sub>plastic</sub> (%)
		k <sub>1</sub>	k <sub>2</sub>	k <sub>3</sub>		
S6M	94.8	442.80	1.324	-0.522	0.988	0.041
S1Y	184	1182.63	0.797	-0.374	0.987	0.039
S2Y	98.4	522.76	1.077	-0.396	0.990	0.055
GAB1	186	1096.53	0.983	-0.489	0.980	0.077
GAB2	249	1594.21	0.864	-0.487	0.988	0.043
GAB3	87	406.20	1.114	-0.135	0.987	0.066
GAB4	130	765.36	0.950	-0.426	0.979	0.078
GAB5	117	647.50	0.995	-0.354	0.996	0.060

Note: S: Steel slag, GAB: Graded aggregate base, SM<sub>R</sub>: Summary resilient modulus.

D 7382. All materials were compacted in six layers at their optimum moisture contents and maximum dry unit weights.

A Geocomp LoadTrac-II loading frame and associated hydraulic power unit system was used to load the specimens (Fig. 2). A conditioning stage was performed on the specimens before actual test loading under the same confining and axial stress of 103 kPa for 500 repetitions. The confining stress was constrained between 20.7 and 138 kPa during the loading stages, while the deviator stress was raised from 20.7 kPa to 275.8 kPa with 100 repetitions at each step. Resilient modulus 5.0 software was used to keep track of the loading sequence, confining pressure, and data acquisition. External linear variable displacement transducers (LVDTs) with a measurement capacity of 50.8 mm were utilized to measure the deformations. In order to obtain the resilient

modulus for each load sequence, the average moduli from the last five cycles of the corresponding sequence were calculated. The following model in the Mechanistic-Empirical Pavement Design Guide (MEPDG) [36, 37] was used to calculate the resilient moduli:

$$M_R = k_1 \times P_a \times \left(\frac{\theta}{P_a}\right)^{k_2} \times \left(\frac{\tau_{oct}}{P_a} + 1\right)^{k_3} \quad (1)$$

where M<sup>R</sup>= resilient modulus; k<sub>1</sub>; k<sub>2</sub>, and k<sub>3</sub> are constants; θ = bulk stress (σ<sub>1</sub> + σ<sub>2</sub> + σ<sub>3</sub>); P<sub>a</sub> = atmospheric pressure. τ<sub>oct</sub> is octahedral stress depending on the principal stresses acting on the sample and calculated as follows:

$$\tau_{oct} = \frac{1}{3} \sqrt{(\sigma_1 - \sigma_2)^2 + (\sigma_1 - \sigma_3)^2 + (\sigma_2 - \sigma_3)^2} \quad (2)$$

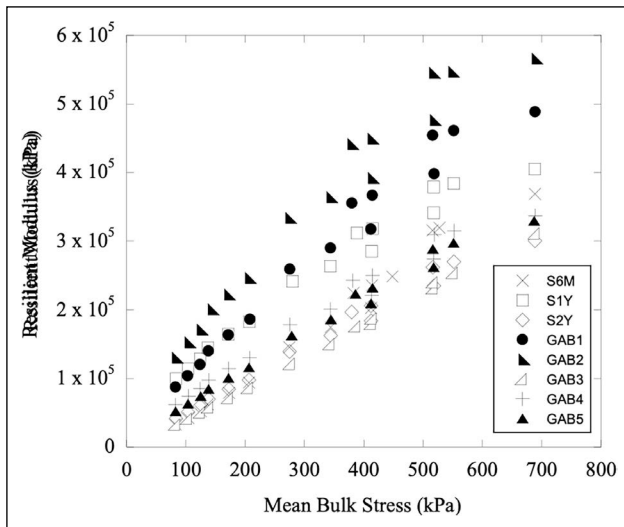


**Figure 3.** Resilient moduli of GABs and steel slags at different loading sequences.

The resilient modulus data at a bulk stress of 208 kPa computed by National Cooperative Highway Research Program 1-28A was named the summary resilient modulus ( $SM_R$ ) ([38]). The resilient modulus test results are summarized in Table 4 and Figure 3.

### 3.2. Permanent Deformation Test

In order to obtain the plastic strain characteristics of the specimens, a battery of permanent deformation tests was performed by AASHTO T-307 ([35]). The samples were subjected to the same preconditioning steps; however, after the preconditioning stage, the specimens were subjected to 10,000 load repetitions under 103.4 kPa confining pressure and 206.8 kPa deviator stresses in order to measure the permanent deformations. Permanent deformation tests were terminated after 10,000 load repetitions were completed or a plastic strain of 5% was reached.

## 4. RESULTS

### 4.1. Resilient Modulus Test

The results of the resilient moduli test for all samples are presented in Figure 3 and Table 4. There is a near-linear relationship between bulk stress and resilient modulus, as observed in earlier studies [24, 27, 39–43]. The data in Figure 3 and Table 4 indicate that the  $SM_R$  of steel slag (S) is comparable to those of GAB materials. The  $SM_R$  values obtained for steel slag samples agree with the findings of [12] but are slightly lower than those reported by [44]. However, it should be noted that the latter study used an empirical equation to obtain  $M_R$  from the laboratory CBR test results. Although the steel slag samples have a lower gravel fraction, higher fines content, and higher optimum moisture content, their resilient moduli remained within the range of resilient moduli of traditional GAB materials. This phe-

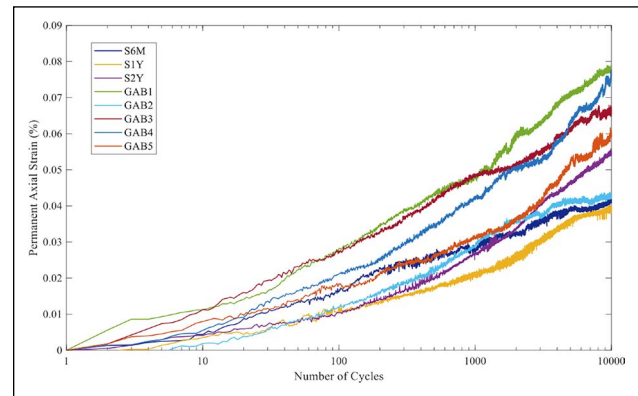


**Figure 4.** Permanent strains of the GABs and steel slags.

nomenon might be due to their relatively higher angularity and roughness [12, 24], even though such measurements were not made in the current study [45] reported that the resilient modulus of steel slag is significantly dependent on deviator stress, and the fine fraction of steel slag may be responsible for the observed behavior. No apparent correlation exists between the aging period and resilient modulus since the maximum and minimum  $SM_R$  was observed for S1Y and S6M, respectively. However, Table 4 indicates that the highest unit weight results in the lowest  $SM_R$ , agreeing with the findings of [46].

Table 4 indicates that all  $k_3$  values are negative and vary between -0.135 and -0.522, most probably because the granular materials used in this study are affected by bulk stress [24]. Furthermore, the results show that the resilient moduli values depend on the bulk stress level applied. At the lower bulk stress levels (100–500 kPa), the minimum and maximum  $M_R$  were computed for GAB2 and GAB3, respectively, while at the higher bulk stress levels (600–700 kPa), the minimum  $M_R$  was calculated for S2Y.

### 4.2. Permanent Deformation Test

Table 4 and Figure 4 show the plastic strain of all materials used in the current study. GAB1 has the maximum plastic strain (0.078%), whereas S1Y has the minimum plastic strain (0.039%) after 10,000 repeated loading cycles. In general, steel slags yield lower plastic strains when compared with the GAB materials ( $\epsilon = 0.039$ –0.055 versus 0.043–0.078), suggesting a better performance for the slags under a specific load for the long term. Upon subjected to 10,000 repeated cycles of loading, GAB4 shows the maximum plastic strain (0.078%), whereas GAB2 has the minimum plastic strain (0.043%) among the GABs tested, which may be attributed to the gravel and acceptable content of these two GABs (Table 1). GAB4 has a relatively higher gravel content (58% versus 46.8%) and lower fines (5.3% versus 8.6%) than GAB2, resulting in a larger void ratio for GAB4. The large voids between the particles and lack of fines may have resulted in more significant deformation during repeated loading [47].

## 5. CONCLUSIONS

A series of laboratory tests were conducted to study the resilient modulus and permanent deformations of a steel slag material and to compare the measured values to those of natural aggregates. In addition, the swelling potentials of pure slag, as well as Bitumen-coated slag particles were determined in accelerated swelling tests. The following conclusions can be drawn from the findings of this study:

- Resilient moduli of steel slag with different aging properties were comparable to those of traditional graded aggregate base materials. Although the tested steel slag samples have lower gravel fraction, higher fines content, and higher optimum moisture content, the  $SM_R$  of steel slag samples remained within the range of values for graded aggregate base materials.
- In general, steel slag materials yielded lower plastic strains as compared to GAB materials. These results show that steel slag performs better than GAB under a specific load for the long term.
- All three steel slag materials with different aging properties exceeded the 0.5% swell limit set by ASTM D 2940 at seven days.
- The aging process did not seem to influence the ultimate swelling of steel slags, contrary to findings reported in past studies. Surface area and fines content may be the dominant factors for Ca-release potential and measured swelling ratios.
- Even though the mechanical test results showed that steel slags could be potentially used instead of earthen aggregates, the pollution and pH characteristics of steel slags must be evaluated in the laboratory and field.

## ACKNOWLEDGEMENTS

The research reported in this paper was financially supported by the U.S. Department of Transportation National Transportation Center (NTC) and the Maryland State Highway Administration (SHA). Endorsement by NTC, SHA, or the steel slag supplier is not implied and should not be assumed.

## ETHICS

There are no ethical issues with the publication of this manuscript.

## DATA AVAILABILITY STATEMENT

The authors confirm that the data that supports the findings of this study are available within the article. Raw data that support the finding of this study are available from the corresponding author, upon reasonable request.

## CONFLICT OF INTEREST

The author declare that they have no conflict of interest.

## FINANCIAL DISCLOSURE

The authors declared that this study has received no financial support.

## PEER-REVIEW

Externally peer-reviewed.

## REFERENCES

- [1] Dayioglu, A. Y., Aydilek, A. H., Cimen, O., & Cimen, M. (2018). Trace metal leaching from steel slag used in structural fills. *Journal of Geotechnical and Geoenvironmental Engineering*, 144(12), Article 04018089. [\[CrossRef\]](#)
- [2] Dayioglu, A. Y., & Aydilek, A. H. (2019). Effect of pH and subgrade type on trace-metal leaching from steel-slag embankments into groundwater. *Journal of Materials in Civil Engineering*, 31(8), Article 04019149. [\[CrossRef\]](#)
- [3] US Geological Survey. (2021). Iron and steel slag statistics. *Miner. Commod. Summ. Slag-Iron Steel* Washington, DC., no. 703, pp. 86–87, 2021. <https://www.usgs.gov/centers/national-minerals-information-center/iron-and-steel-slag-statistics-and-information>
- [4] Tsakiridis, P. E., Papadimitriou, G. D., Tsivilis, S., & Koroneos, C. (2008). Utilization of steel slag for Portland cement clinker production. *Journal of Hazardous Materials*, 152(2), 805–811. [\[CrossRef\]](#)
- [5] Pellegrino, C., & Gaddo, V. (2009). Mechanical and durability characteristics of concrete containing EAF slag as aggregate. *Cement and Concrete Composites*, 31(9), 663–671. [\[CrossRef\]](#)
- [6] Gao, J. T., Li, S. Q., Zhang, Y. T., Zhang, Y. L., Chen, P. Y., & Shen, P. (2011). Process of re-resourcing of converter slag. *Journal of Iron and Steel Research International*, 18(12), 32–39. [\[CrossRef\]](#)
- [7] Brand, A. S., & Roesler, J. R. (2015). Steel furnace slag aggregate expansion and hardened concrete properties. *Cement and Concrete Composites*, 60, 1–9. [\[CrossRef\]](#)
- [8] Devi, V. S., & Gnanavel, B. K. (2014). Properties of concrete manufactured using steel slag. *Procedia Engineering*, 97, 95–104. [\[CrossRef\]](#)
- [9] Xue, P., He, D., Xu, A., Gu, Z., Yang, Q., Engström, F., & Björkman, B. (2017). Modification of industrial BOF slag: Formation of MgFe<sub>2</sub>O<sub>4</sub> and recycling of iron. *Journal of Alloys and Compounds*, 712, 640–648. [\[CrossRef\]](#)
- [10] Li, Y., & Dai, W. B. (2018). Modifying hot slag and converting it into value-added materials: a review. *Journal of Cleaner Production*, 175, 176–189. [\[CrossRef\]](#)
- [11] He, Z., Hu, X., & Chou, K. C. (2022). Synergetic modification of industrial basic oxygen furnace slag and copper slag for efficient iron recovery. *Process Safety and Environmental Protection*, 165, 487–495. [\[CrossRef\]](#)

- [12] Rohde, L., Peres Núñez, W., & Augusto Pereira Ceratti, J. (2003). Electric arc furnace steel slag: base material for low-volume roads. *Transportation Research Record*, 1819(1), 201–207. [\[CrossRef\]](#)
- [13] Ahmedzade, P., & Sengoz, B. (2009). Evaluation of steel slag coarse aggregate in hot mix asphalt concrete. *Journal of Hazardous Materials*, 165(1-3), 300–305. [\[CrossRef\]](#)
- [14] Pasetto, M., & Baldo, N. (2010). Experimental evaluation of high performance base course and road base asphalt concrete with electric arc furnace steel slags. *Journal of Hazardous Materials*, 181(1-3), 938–948. [\[CrossRef\]](#)
- [15] Amelian, S., Manian, M., Abtahi, S. M., & Goli, A. (2018). Moisture sensitivity and mechanical performance assessment of warm mix asphalt containing by-product steel slag. *Journal of Cleaner Production*, 176, 329–337. [\[CrossRef\]](#)
- [16] Liu, J., Xu, J., Liu, Q., Wang, S., & Yu, B. (2022). Steel slag for roadway construction: a review of material characteristics and application mechanisms. *Journal of Materials in Civil Engineering*, 34(6), Article 03122001. [\[CrossRef\]](#)
- [17] Ameri, M., & Behnood, A. (2012). Laboratory studies to investigate the properties of CIR mixes containing steel slag as a substitute for virgin aggregates. *Construction and Building Materials*, 26(1), 475–480. [\[CrossRef\]](#)
- [18] Maghool, F., Arulrajah, A., Du, Y. J., Horpibulsuk, S., & Chinkulkijniwat, A. (2017). Environmental impacts of utilizing waste steel slag aggregates as recycled road construction materials. *Clean Technologies and Environmental Policy*, 19, 949–958. [\[CrossRef\]](#)
- [19] Shi, C., & Day, R. L. (1999). Early strength development and hydration of alkali-activated blast furnace slag/fly ash blends. *Advances in Cement Research*, 11(4), 189–196. [\[CrossRef\]](#)
- [20] Shi, C., & Qian, J. (2000). High performance cementing materials from industrial slags—a review. *Resources, Conservation and Recycling*, 29(3), 195–207. [\[CrossRef\]](#)
- [21] Wang, G., Wang, Y., & Gao, Z. (2010). Use of steel slag as a granular material: Volume expansion prediction and usability criteria. *Journal of Hazardous Materials*, 184(1-3), 555–560. [\[CrossRef\]](#)
- [22] Ozkok, E., Davis, A. P., & Aydilek, A. H. (2016). Treatment methods for mitigation of high alkalinity in leachates of aged steel slag. *Journal of Environmental Engineering*, 142(2), Article 04015063. [\[CrossRef\]](#)
- [23] Dayioglu, A. Y., & Aydilek, A. H. (2017). Evaluation of mitigation techniques for the expansive behavior of steel slag. *Geotechnical Frontiers* 2017, 360–368. [\[CrossRef\]](#)
- [24] Stolle, D., Guo, P., & Liu, Y. (2009). Resilient modulus properties of granular highway materials. *Canadian Journal of Civil Engineering*, 36(4), 639–654. [\[CrossRef\]](#)
- [25] Khogali, W. E., & Mohamed, E. H. H. (2004). Novel approach for characterization of unbound materials. *Transportation Research Record*, 1874(1), 38–46. [\[CrossRef\]](#)
- [26] Mishra, D., & Tutumluer, E. (2012). Aggregate physical properties affecting modulus and deformation characteristics of unsurfaced pavements. *Journal of Materials in Civil Engineering*, 24(9), 1144–1152. [\[CrossRef\]](#)
- [27] Haider, I., Kaya, Z., Cetin, A., Hatipoglu, M., Cetin, B., & Aydilek, A. H. (2014). Drainage and mechanical behavior of highway base materials. *Journal of Irrigation and Drainage Engineering*, 140(6), Article 04014012. [\[CrossRef\]](#)
- [28] Hatipoglu, M., Cetin, B., & Aydilek, A. H. (2020). Effects of fines content on hydraulic and mechanical performance of unbound granular base aggregates. *Journal of Transportation Engineering, Part B: Pavements*, 146(1), Article 04019036. [\[CrossRef\]](#)
- [29] Tutumluer, E., & Pan, T. (2008). Aggregate morphology affecting strength and permanent deformation behavior of unbound aggregate materials. *Journal of Materials in Civil Engineering*, 20(9), 617–627. [\[CrossRef\]](#)
- [30] Kvasnak, A., West, R., Michael, J., Loria, L., Hajj, E. Y., & Tran, N. (2010). Bulk specific gravity of reclaimed asphalt pavement aggregate: Evaluating the effect on voids in mineral aggregate. *Transportation Research Record*, 2180(1), 30–35. [\[CrossRef\]](#)
- [31] Deniz, D., Tutumluer, E., & Popovics, J. S. (2010). Evaluation of expansive characteristics of reclaimed asphalt pavement and virgin aggregate used as base materials. *Transportation Research Record*, 2167(1), 10–17. [\[CrossRef\]](#)
- [32] Yildirim, I. Z., & Prezzi, M. Chemical, mineralogical, and morphological properties of steel slag. *Advances in Civil Engineering*, 2011, Article 463638. [\[CrossRef\]](#)
- [33] AASHTO M145-91. (2007). American Association of State Highway and Transportation Officials. Classification of Soils and Soil-Aggregate Mixtures for Highway Construction Purposes. Washington DC: American Association of State Highway and Transportation Officials.
- [34] Dayioglu, A. Y., Aydilek, A. H., & Cetin, B. (2014). Preventing swelling and decreasing alkalinity of steel slags used in highway infrastructures. *Transportation Research Record*, 2401(1), 52–57. [\[CrossRef\]](#)

- [35] AASHTO T 307-99. (2007). Standart Method of Testing for: Determining the Resilient Modulus of Soils and Aggregate Materials.” p. 40, <https://www.scribd.com/document/378718757/2007-Standard-Method-of-Test-for-Determining-the-Resilient-Modulus-of-Soils-and-Aggregate-Materials#>
- [36] R. G. Hicks. (2004). NCHRP 01-37 Guide for mechanistic-empirical design of new and rehabilitated pavement structures. National Cooperative Highway Research Program 1-47A Report. Transportation Research Board, National Research Council, Washington, DC.
- [37] Kancherla, A. (2004). Resilient modulus and permanent deformation testing of unbound granular materials [Unpublished doctoral dissertation]. Texas A&M University.
- [38] Witczak, M. W. (1998). Harmonized test methods for laboratory determination of resilient modulus for flexible pavement design (NCHRP Report 1-28A). National Cooperative Highway Research Program Transportation Research Board National Research Council.
- [39] Cetin, B., Aydilek, A. H., & Guney, Y. (2010). Stabilization of recycled base materials with high carbon fly ash. *Resources, Conservation and Recycling*, 54(11), 878–892. [\[CrossRef\]](#)
- [40] Arulrajah, A., Piratheepan, J., Aatheesan, T., & Bo, M. W. (2011). Geotechnical properties of recycled crushed brick in pavement applications. *Journal of Materials in Civil Engineering*, 23(10), 1444–1452. [\[CrossRef\]](#)
- [41] Arulrajah, A., Piratheepan, J., Disfani, M. M., & Bo, M. W. (2013). Resilient moduli response of recycled construction and demolition materials in pavement subbase applications. *Journal of Materials in Civil Engineering*, 25(12), 1920–1928. [\[CrossRef\]](#)
- [42] Patel, S., & Shahu, J. T. (2016). Resilient response and permanent strain of steel slag-fly ash-dolime mix. *Journal of Materials in Civil Engineering*, 28(10), Article 04016106. [\[CrossRef\]](#)
- [43] Bestgen, J. O., Hatipoglu, M., Cetin, B., & Aydilek, A. H. (2016). Mechanical and environmental suitability of recycled concrete aggregate as a highway base material. *Journal of Materials in Civil Engineering*, 28(9), Article 04016067. [\[CrossRef\]](#)
- [44] Sas, W., Głuchowski, A., Radziemska, M., Dzięcioł, J., & Szymański, A. (2015). Environmental and geotechnical assessment of the steel slags as a material for road structure. *Materials*, 8(8), 4857–4875. [\[CrossRef\]](#)
- [45] Yoshida, N., Kimura, H., & Miyahara, T. (2010). Comparison of mechanical characteristics of slag base-course materials produced by various iron and steel manufacturers in Japan. *Proceedings of 11th international conference on asphalt pavements* (pp. 2342-2352). International Society for Asphalt Pavements.
- [46] Pacheco, L. G., & Nazarian, S. (2011). Impact of moisture content and density on stiffness-based acceptance of geomaterials. *Transportation Research Record*, 2212(1), 1–13. [\[CrossRef\]](#)
- [47] Xiao, Y., Tutumluer, E., Qian, Y., & Siekmeier, J. A. (2012). Gradation effects influencing mechanical properties of aggregate base–granular subbase materials in Minnesota. *Transportation Research Record*, 2267(1), 14–26. [\[CrossRef\]](#)